AIAA Aviation
22-26 June 2015, Dallas, TX
15th AIAA Aviation Technology, Integration, and Operations Conference

Strategic time-based metering that assures separation for integrated operations in a terminal airspace

A. Sadovsky, M. Jastrzebski

This paper reports an algorithm for strategic time-based metering of air traffic arriving and departing from a large ($\sim$ tens of nautical miles) area (called here, *the commitment region*) around an airport or metroplex. The algorithm assures separation continuously in time and avoids a dictation of intent to an aircraft crew. This is accomplished by allowing an aircraft (specifically, its Flight Management System) to specify, and commit to, an intended route and ground speed profile along that route within the commitment region, and by supplying the time at which to enter the region to the aircraft crew. The airspace that comprises the commitment region need not be confined to the terminal airspace and can include some of the en-route space: the size and shape of the commitment region are parameters in the algorithm. An exact formula for including speed profile uncertainty in the algorithm is provided. The algorithm is applied to a number of data sets recorded during actual air traffic operations in the Southern California TRACON in July of 2014 and the Atlanta TRACON in November and December of 2013. The results of the numerical simulations indicate that the algorithm succeeds at keeping the aircraft separated, but introduces, in its current implementation, more separation than that observed in actual operations. This excess separation can be reduced by modeling more accurately the Visual Flight Rules separation practices, a direction for future research.

I. Introduction

Air Traffic Operations (ATO) in terminal airspace differ from those in en route airspace in several key aspects [1]. Two such distinctions are, *(i)*, the abundance in a terminal airspace of merging arrival routes and shortage of room for maneuvers, for absorbing delay, such as holding patterns, and, *(ii)*, the absence in a terminal airspace of a full route specification for an arriving flight all the way to the runway; see, e.g., Ref. [1, section II.B.1]. These characteristics of current ATO in terminal airspace limit the means available to Air Traffic Control (ATC) to enforce the Federal Aviation Administration's (FAA) requirement of separation assurance [2]. This limitation also affects areas of research in Air Traffic Management (ATM) that involves separation assurance; in particular, research aimed at providing automated decision support for ATC in terminal airspace.

Two areas of such research are Precision Air Traffic Operations in terminal airspace [3, 4, 5, 6, 1, 7], including the research sub-area called Time Advance [8, 9], and Integrated Arrival-Departure Operations [10] (see also the references cited in Ref. [10]). To have value in the field, an automated decision support solution sought in these areas must, in some way, reach an acceptable compromise between the interdependent and, in part, competing goals listed in Table 1. Being interdependent, these goals must be pursued simultaneously; for example, if the optimization

Table 1: Operational goals pursued in the design of an automated decision support solution for ATM.

* operational safety
* schedule efficiency
* actual executability of the proposed solutions
* adaptability and robustness of the proposed solutions to unpredictable perturbations (e.g., wind or lapses in runway availability)
* correctness and sufficiently fast performance of the algorithms underlying the automation

and separation assurance for an ATO are addressed consecutively, not concurrently, then the latter stage (separation assurance) may disturb the results of the former (optimality). Similarly, the last goal in Table 1 is concerned with

how reliable and timely the automation will be in its function. This goal is, hence, closely related to the first goal (operational safety). A detailed discussion of these goals and challenges is found in [1].

The objective of this paper is automated decision support for fulfilling simultaneously two tasks, scheduling and separation assurance (treated separately in most of the literature). The algorithm developed in this paper is an attempt provide this capability. Aircraft separation is assured continuously in time. The input to the algorithm consists of: a region (of a diameter on the scale of tens of nautical miles) surrounding a given airport or metroplex; the aerial route network in that region; a sequence of flights that are arrivals to, and departures from, that region; and the route and speed profile intent of each flight. As output, the algorithm computes for each flight, the time instant at which that flight should enter the region (for departing flights, entrance into the region is defined as the takeoff) so that, if all flights hold to their intended routes and (with some error margin) speed profiles, separation will be assured within the region at all times during the ATO.

The following facts were taken into account during the design of the algorithm. Inside a Terminal Radar Approach Control (TRACON) [1] airspace, aircraft speeds are subject to a number of restrictions. Some of these are mandated by the FAA, and others are a matter of preferred practice. Specifically, anecdotal knowledge obtained by the authors from a former controller suggests that controllers generally prefer to hold the flights arriving in a TRACON to certain speed profiles. This preference, controllers believe, simplifies the task of visual assessment of aircraft separation. It is, therefore, common in current ATO that an aircraft be committed to following, at least with a certain degree of accuracy, a specified speed profile while inside the TRACON. Furthermore, ATC and representatives of commercial FMS manufacturers [11] dislike a system wherein intent is dictated to ATC or to aircraft crew. (For more details on attempts to design such systems, see Section II.) ATC and crews prefer, instead, that the aircraft use its Flight Management System (FMS) to compute intent based on the aircraft's individual characteristics and the airline's preferences. The main merit of the algorithm proposed herein is, therefore, twofold: it accommodates, rather than dictates, the intent of the aircraft, and assures separation in continuous time.

The algorithm is described in Section III. It solves a class of problems wherein it is assumed that the given flights are sequenced and routed. If this assumption is dropped, the problem becomes an instance of the *Asymmetric Traveling Salesman Problem with Precedence Constraints (ATSPPC)* [12] The ATSPPC is discussed briefly in Section VI.

The algorithm is tested on a data set that consists of radar track recordings of actual flights. The data and the test results are described in Sections IV and V. A computation necessary in each iteration of the algorithm is described in a separate Subsection, B, of III. A formula for estimating the sensitivity of solutions to various perturbations to the aircraft's speed (e.g., wind) is derived in Appendix A. Such perturbations are not simulated in the numerical examples provided in this paper.

II. Prior research and its lessons

A trend in ATM research that began approximately in the early 1970's (see Ref. [1, section V] for a comprehensive review and list of citations) has been to compute air traffic schedules, including those optimized to an objective function, using a model with the spatial variables being discrete (as opposed to successively refined discretizations of a model with continuous spatial variables). This trend can be traced to the introduction of the concept of *time-based metering* [13, 14] for en-route air traffic that led to the development of the Traffic Management Advisor (TMA) [15].

Recent literature also documents attempts to research automation of terminal air traffic management using the discrete variable modeling approach. The two most prevalent approaches in the algorithms based on such models (see, e.g., Ref. [16], the references cited therein, and the research review in [1, section V]) are Mixed-Integer Linear Programming and Dynamic Programming (see, e.g., Ref. [17]). Almost all these efforts, however, are various attempts to model air traffic as a *network flow* [18] using an inherently discrete model. In algorithms based on such models, however, aircraft separation is enforced only at a finite number of airspace waypoints and runways, and hence have questionable applicability to the terminal airspace setting. Many of the solutions were obtained for problems concerning en-route (not terminal) air traffic and are, consequently, concerned primarily with traffic flow, assuming there is enough space to assure separation and conduct the necessary aircraft holding procedures to absorb delay. Some of these models rely on heuristics-based algorithms that are difficult to verify for correctness and to analyze for performance. The assumption of sufficient space, however, often fails in terminal airspace, and the complexity and incomplete understanding of an algorithm casts doubt on its applicability in real time.

The more recent works, e.g. [9, 4, 5, 8, 6, 19], have, by contrast, attempted to model the motion of the aircraft and to enforce separation continuously in time. These works, however, tend to run into the challenge of unrealistic computed speed profiles, which hinders executability in real time. The alternative of imposing sufficient constraints to obtain executable speed profiles, on the other hand, is hindered by the absence of uniform standards of aircraft performance and airport regulations, and is likely to increase the computational demand substantially, once again

compromising real-time applicability.

In summary, research experience suggests that, when pursuing the goals listed in Table 1, a modeling effort aimed at designing and deploying an automation system tends to become a tradeoff between combinatorial (i.e., growing factorially with problem size) complexity, model fidelity, and the degree to which the algorithms used are currently understood. The approach formulated in the present paper gives priority to operational safety (by assuring separation continuously in time) and executability, and yet achieves computational scalability to manage up to tens of aircraft.

III. The algorithm

A. Input and output

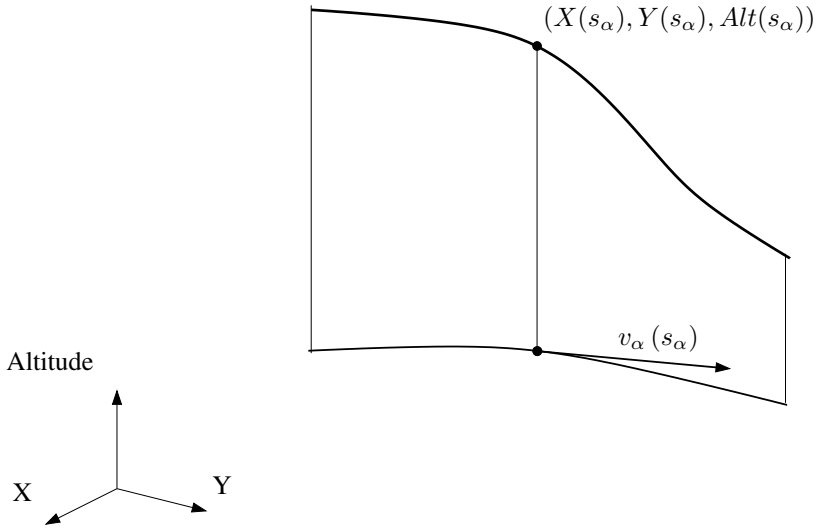

Figure 1: A projection of the route, and of a tangent velocity vector, onto the XY-coordinate (flat Earth) plane.

The input to the algorithm consists of the following data:

(i) An airspace region C, henceforth called the *commitment region* (for reasons explained below), that includes an airport or a metroplex.

(ii) A sequence of aircraft, indexed $\alpha = 1, 2, \ldots, A$ in the pre-determined order of entering the commitment region C. Entrance into C for a departing flight is defined as departing from an airport in C. Here A denotes the total number of flights.

(iii) For each flight α, a route contained entirely in C, parameterized by the ground arc length s_α of the route's projection onto the flat Earth (see Figure 1), and a ground speed profile $v_\alpha(s_\alpha)$ specified, with some margin of error, for that entire route and assumed to be sufficiently smooth to assure the existence of all the derivatives required in subsequent calculations.

A notional illustration of the commitment region C is given in figure 2. The two routes shown are a departure (left) and an arrival (right). The airport or metroplex is shown as a hatched circle. The portion of each route contained in the commitment region is shown thicker than the route outside the region. The diameter of the region is on the scale of tens of NMI. The algorithm will apply to an integrated ATO; i.e., one that involves both arrivals and departures. A specific example in which the commitment region C is a circular cylinder of radius 60 NMI, with a the bottom base centered at the Los Angeles International Airport, is shown in Figure 3.

The specification of s_α, of $v_\alpha(s_\alpha)$, and of the time t_α^0 at which flight α enters C at location $s_\alpha = s_\alpha^0$ completely determines the solution of the initial value problem

$$\frac{ds_\alpha}{dt} = v_\alpha(s_\alpha), \quad s_\alpha\left(t_\alpha^0\right) = s_\alpha^0, \tag{1}$$

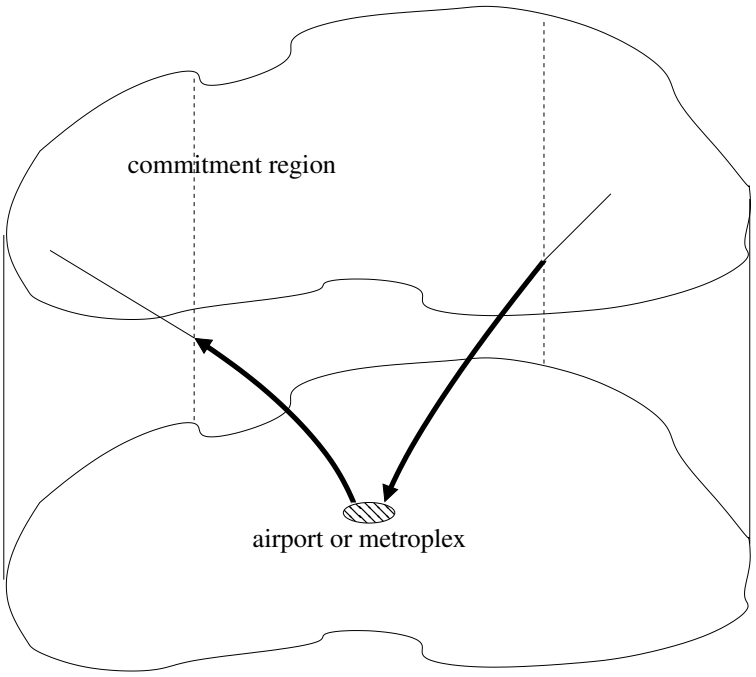

Figure 2: A notional illustration of a commitment region, shown here as a cylinder with one base on the approximately flat Earth surface.

which describes the motion of the aircraft in C. Knowledge of this motion for each aircraft allows the computation of minimal required differences between two consecutive entrance times $t^0_{\alpha_1}, t^0_{\alpha_2}$ required to assure that the two aircraft remain separated at all times while both are in C. This computation is described in detail in Section B. See, in particular, the notation $\triangle t(\alpha_2, \alpha_1)$, defined by the right-hand side of (5), for the minimal required time gap between aircraft α_1, α_2 entering C, in that order, for these two aircraft to be separated at all times.

The output of the algorithm is a sequence $t^0_\alpha,\ \alpha = 1, 2, \ldots, A$, defined by the following recursion:

$$t^0_\alpha = \max\left\{ \quad t^0_{\alpha-1} + \triangle t(\alpha, \alpha-1), \quad t^0_{\alpha-2} + \triangle t(\alpha, \alpha-2), \quad \ldots, \quad t^0_1 + \triangle t(\alpha, 1) \quad \right\}. \tag{2}$$

B. Computation of the minimal difference between consecutive entrance times

From the ordinary differential equations in (1), one can compute, for each aircraft pair α_1, α_2, the region in the $s_{\alpha_1} s_{\alpha_2}$ - coordinate plane consisting of all points $(s_{\alpha_1}, s_{\alpha_2})$ that correspond to the two aircraft violating separation. This region will be denoted $R(\alpha_1, \alpha_2)$; see Figure 4. (For the details of this computation, see [4, 5, 6].) Furthermore, assuming aircraft α_1 enters C at time $t = 0$, and aircraft α_2 does so at a later time $\triangle t > 0$, one obtains a point

$$\big(s_{\alpha_1}(\triangle t), s_{\alpha_2}(\triangle t)\big) \tag{3}$$

in the $s_{\alpha_1} s_{\alpha_2}$ - coordinate plane which can serve as the initial state for the system

$$\frac{d}{dt}\begin{bmatrix} s_{\alpha_1} \\ s_{\alpha_2} \end{bmatrix} = \begin{bmatrix} v_{\alpha_1}(s_{\alpha_1}) \\ v_{\alpha_2}(s_{\alpha_2}) \end{bmatrix}. \tag{4}$$

Equation system (4) and state (3) together constitute an *initial value problem (IVP)* that, with certain smoothness assumptions on the ground speed profiles $v(\cdot)$, has a unique solution. (Figure 4 gives a notional illustration of such a solution.) One can therefore determine all such $\triangle t$ that the solution $(s_{\alpha_1}(t), s_{\alpha_1}(t))_{t \geq \triangle t}$ of the IVP never enters the interior of $R(\alpha_1, \alpha_2)$, i.e. corresponds to a separation-compliant motion of the aircraft pair.

The minimal required value of $\triangle t$ will be denoted by $\triangle t(\alpha_2, \alpha_1)$. It is computed herein using the following method.

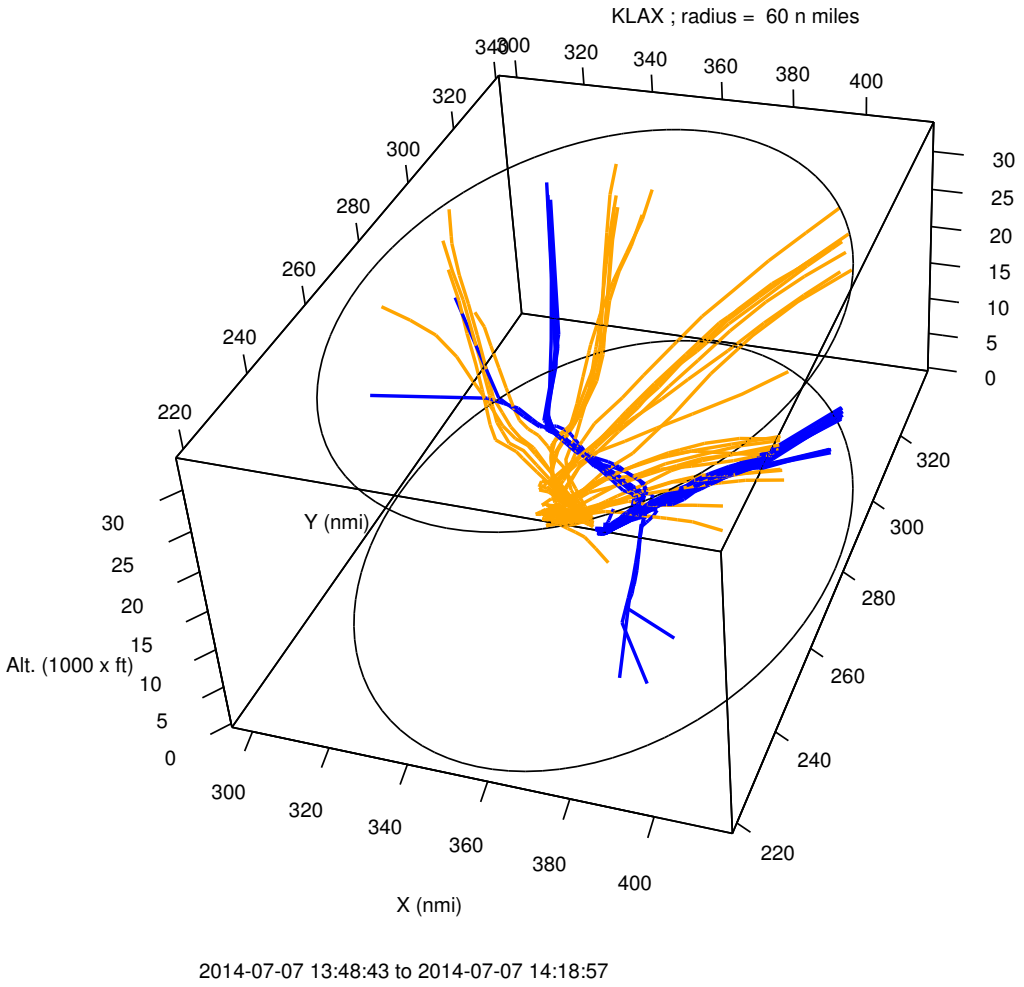

Figure 3: An example of a commitment region at the Los Angeles International Airport (here C is a circular cylinder of radius 60 NMI). The colored curves show radar track hit data for arrivals (blue) and departures (orange) that entered C in the time window from 1:48 PM to 2:18 PM on July 7, 2014.

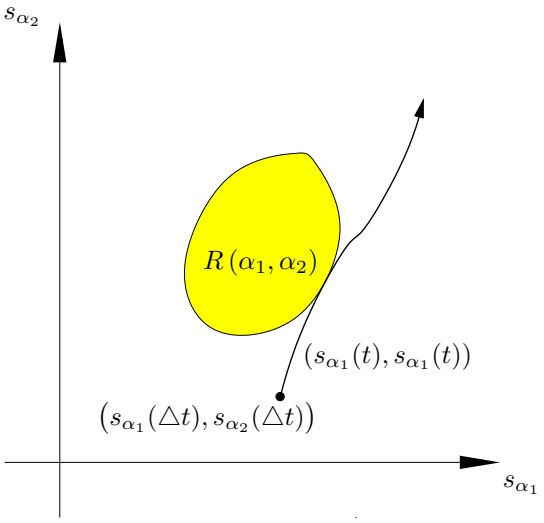

Figure 4: A notional illustration of a phase curve $(s_{\alpha_1}(t), s_{\alpha_1}(t))$ that avoids the interior of the set $R(\alpha_1, \alpha_2)$ separation-violating states.

Sample the trajectories of the two aircraft at points

$$s^0_{\alpha_1},\ s^1_{\alpha_1},\ s^2_{\alpha_1},\ \dots\ ,$$

$$s^0_{\alpha_2},\ s^1_{\alpha_2},\ s^2_{\alpha_2},\ \dots\ ,$$

with every two consecutive points on a trajectory being some fixed distance, h, apart:

$$s^{i+1}_{\alpha_1} - s^i_{\alpha_1} = h, \quad s^{j+1}_{\alpha_2} - s^j_{\alpha_2} = h, \quad i, j = 0, 1, \dots\ .$$

For each pair $\left(s^i_{\alpha_1}, s^j_{\alpha_2}\right)$ that corresponds to a violation of the separation requirement for the aircraft pair α_1, α_2, determine the corresponding times $t^i_{\alpha_1}, t^j_{\alpha_2}$:

$$s_{\alpha_1}\left(t^i_{\alpha_1}\right) = s^i_{\alpha_1}, \quad s_{\alpha_2}\left(t^j_{\alpha_2}\right) = s^j_{\alpha_2}.$$

The value of $\triangle t(\alpha_2, \alpha_1)$ is chosen to be the largest of the differences $t^j_{\alpha_2} - t^i_{\alpha_1}$:

$$\triangle t(\alpha_2, \alpha_1) = \max_{i,j}\left(t^j_{\alpha_2} - t^i_{\alpha_1}\right) \tag{5}$$

Because the execution of a ground speed profile always contains some error, analysis of sensitivity to such errors is carried out in Appendix A.

IV. Methods

A. Dates and time windows

In the sample solutions shown here, the commitment region C was taken to be a circular cylinder, with the lower base centered at the indicated airport, of radius 60 NMI. The input data are recordings of the actual radar tracks in the Center-TRACON Automation System (CTAS) [14]. The two airports for which data are shown in the figures below are Charlotte Douglas International (CLT) and Los Angeles International (LAX). Each figure showing a data plot is accompanied by a specification (printed above the plots) of the airport and the time window during which the traffic was recorded.

For LAX, the algorithm described in Section III was tested using traffic recording data from July 3 through 5 of 2014. To compare the traffic behavior to that on a date away from a holiday, an analogous test was run on traffic data recorded July 18, 2014. For Charlotte Douglas International (CLT) and Atlanta International (ATL), the algorithm was tested on traffic data from November 27 through 29 (Nov. 28 was the U.S. Thanksgiving holiday). To compare the

traffic behavior to that on a date away from a holiday, an analogous test was run on traffic data recorded on November 20, 2013. On each date, the data were chosen from a midday window, in an attempt to capture a typical traffic density (that has time to build up since early morning) and typical flight conditions (daylight).

B. Data collection method

For each of a number of dates in 2013 and 2014, a collection of 50 flights recorded in the track data entered the commitment region during the specified time window. The flights were sampled in the order of entering the commitment region. The flights in which the altitude was not a monotonically increasing or decreasing function of time (i.e., flights that were not a clear arrival and not a clear departure) and did not reach both the airport and the boundary of the commitment region were discarded. (The monotonicity was measured as statistical correlation between the recorded trajectory and a theoretical linear trajectory.) A failure to classify the flight as either a departure or an arrival using this method has several possible explanations in terms of actual operations. One explanation is that the flight experienced a missed approach. Another is that radar track data on the same flight collected by different radars, or collected past the landing moment of an arriving flight, may contain spurious artifacts (e.g., poor alignment between the track hits).

The sampling continued until the total number of flights reached 50. The number of flights that ended up being discarded in this process is given in each figure's top section.

All the times of entry into the commitment region, both actual and computed, are given in offset UNIX time recorded in the CTAS file. The time is the number of seconds elapsed since a time instant specific to the operation on that date.

C. How the algorithm was tested on data

In the analysis carried out, each flight's path and speed profile, as recorded in the CTAS, was assumed to coincide with the flight's (actually unknown) intent. For these assumed intents, the algorithm described in Section III was run to compute the minimally spaced separation-compliant times of entering the commitment region, with the first flight entering at the time recorded in the data. The runway separation standards (for in-trail pairs of flights arriving on the same runway) assumed in the algorithm are listed in Table 2. The values in the table were used with scalings described in Section D.

Table 2: The benchmark separation matrix used in the calculations for in-trail arrival pairs on the same runway. The rows are indexed by the possible models of the leading aircraft; e.g., a Boeing 757 arriving directly behind an Extra Heavy Jet must maintain separation of at least 8.0 NMI.

← aircraft behind →								
HJ	LJ	LT	ST	SP	757	XH		
4.0	5.0	5.0	6.0	6.0	5.0	5.0	HJ	
3.5	3.5	3.5	4.0	4.0	3.5	3.5	LJ	↑
3.5	3.5	3.5	4.0	4.0	3.5	3.5	LT	aircraft
3.5	3.5	3.5	3.5	3.5	3.5	3.5	ST	ahead
3.5	3.5	3.5	3.5	3.5	3.5	3.5	SP	↓
4.0	4.0	4.0	5.0	5.0	4.0	4.0	757	
8.0	10.0	10.0	10.0	10.0	8.0	6.0	XH	

Legend:	J	jet
	T	turbopropeller
	H	heavy
	L	light
	S	small
	757	Boeing 757
	X	extra

D. Sources of error

In cases when two flights consecutively arrived on the same runway, the separation standards (given in NMI) listed in Table 2 were used in the computation. For LAX and ATL, enforcement in the algorithm of the standards listed in Table 2 for every pair of in-trail arrivals on the same runway (indicated, perhaps with some error, in the CTAS data) yielded

makespans[a] substantially greater than those recorded live. In the opinion of the authors, as well as of the author of [20] and other SMEs, this is explained by the predominance of VFR (Visual Flight Rules) Approach [20] landings in daylight, which results in separations substantially smaller than those prescribed by the standards in Table 2. To explore this possibility, for LAX and ATL, the algorithm was run, for each of these airports and for each date near or on a holiday, with runway separation standards (see the value 'RWY sep. frac.' in the figure legends) ranging over the following values:

- $1.0\times$ those in Table 2
- $0.75\times$ those in Table 2
- $0.5\times$ those in Table 2

Another source of error is the inaccuracy, in the recorded data, of the data field specifying the flight's arrival runway. The runways specified are the best inference that could be made by the software [14] from the data available about the flight (e.g., the flight plan and subsequent amendments to it).

Because some of these values exceed the minima required at some of the runways, and because some consecutive arrivals on the same runway are visual approaches [20], some of the computed time gaps $\triangle t(\alpha_2, \alpha_1)$ are expected to exceed those recorded in the actual operations. This is, indeed, so for most of the cases presented.

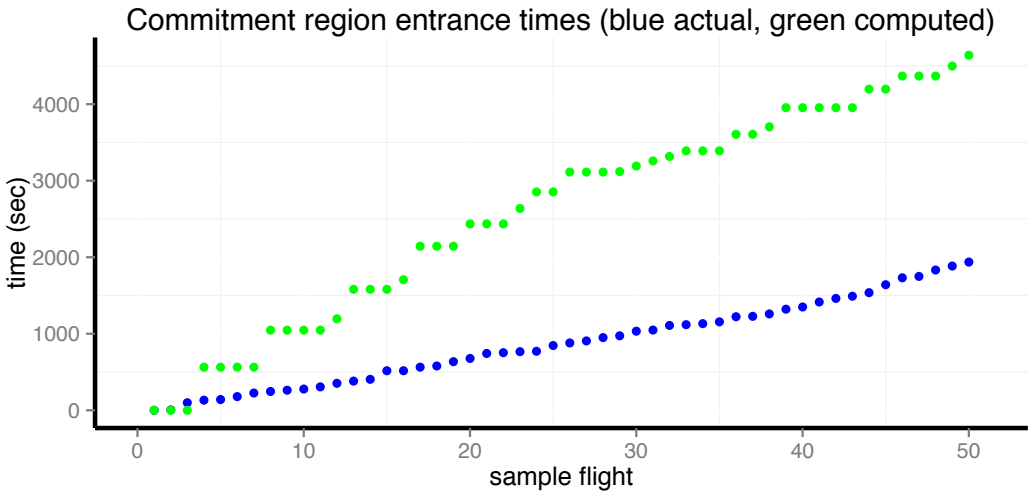

Figure 5: LAX. July 3, 2014. Runway separation standards scaled by factor 1.

Figure 5 shows the results of running the algorithm on one of the dates, with the following details:

LAX: 2014-07-03 13:50:51 to 2014-07-03 14:23:08
2 flights rejected from sample
Separation imposed: 12 to 40 NMI within aiport
Separation minima – lateral: 3 NMI; vertical: 0.164579 NMI
Runway separation fraction enforced: 1
Delay/flt (sec): avg 1722.6 ; std 846.6 ; min: -99 ; max: 2702
Departures: 50 %

V. Results

Table 3 gives a summary of the average delays per flight introduced by the algorithm for the dates and time windows specified in Section IV. This summary suggests the statements listed next:

[a]The *makespan* of an ATO is the total duration of the operation.

Table 3: A summary of the delays per flight introduced by the algorithm. The holidays are marked with an *.

date (yyyy-mm-dd)	airport	RWY sep'n scale	avg. delay/flt (sec)	% departures
2014-07-03	LAX	0.5	1549.5	50
2014-07-03	LAX	0.75	1635.1	50
2014-07-03	LAX	1	1722.6	50
* 2014-07-04	LAX	0.5	563.1	40
* 2014-07-04	LAX	0.75	899.3	40
* 2014-07-04	LAX	1	1084.6	40
2014-07-05	LAX	0.5	1195.9	40
2014-07-05	LAX	0.75	1240.1	40
2014-07-05	LAX	1	1568.1	40
2014-07-18	LAX	0.5	1059.3	50
2014-07-18	LAX	0.75	1100.7	50
2014-07-18	LAX	1	1159.4	50
2013-11-27	ATL	0.5	796.8	50
2013-11-27	ATL	0.75	847.8	50
2013-11-27	ATL	1	963.4	50
* 2013-11-28	ATL	0.5	594.3	50
* 2013-11-28	ATL	0.75	643.8	50
* 2013-11-28	ATL	1	721.4	50
2013-11-29	ATL	0.5	1430.6	50
2013-11-29	ATL	0.75	1433.5	50
2013-11-29	ATL	1	1437.6	50
2013-11-20	ATL	0.5	2811.4	70
2013-11-20	ATL	0.75	2821.7	70
2013-11-20	ATL	1	2843	70
2013-11-27	CLT	0.5	119.1	50
2013-11-27	CLT	0.75	130	50
2013-11-27	CLT	1	142.6	50
* 2013-11-28	CLT	0.5	130.7	40
* 2013-11-28	CLT	0.75	134.7	40
* 2013-11-28	CLT	1	142.7	40
2013-11-29	CLT	0.5	122.8	50
2013-11-29	CLT	0.75	129.3	50
2013-11-29	CLT	1	150.1	50
2013-11-20	CLT	0.5	198	50
2013-11-20	CLT	0.75	207.4	50
2013-11-20	CLT	1	221.1	50

(i) Average delays at LAX and ATL listed in Table 3 exhibit the following patterns:

- At LAX, on non-holiday dates, the average delay per flight introduced by the algorithm at full scale runway separation was at least $1,100$ seconds (~ 18 minutes).
- At ATL, on non-holiday dates, the average delay per flight introduced by the algorithm at full scale runway separation was at least 963 seconds (~ 16 minutes).

Since the algorithm assumes minimal separation (in particular, at the runway), it follows from these patterns that most of the arrivals at LAX and ATL were carried out at separations considerably less than those in the separation matrix in Table 2. This is known to occur widely in practice under VFR [20] and is consistent with the fact that the actual operations were carried out during daylight.

(ii) At LAX and ATL, the average delay per flight introduced by the algorithm appears significantly less on the holiday than on the other days.

Items (i) and (ii) are interpreted collectively at the end of this section.

(iii) At LAX, the average delay introduced by the algorithm exhibits no apparent dependence on the ratio of departures to arrivals within the sample. Specifically, for the computations with the runway separation enforced at full scale, 1.0, the relevant data from Table 3 are reproduced in Table 4.

Table 4: The data on average delay and percentage of departures at LAX with runway fully enforced.

	July 3, 2015	**July 4, 2015**	**July 5, 2015**	**July 18, 2015**
Avg. delay/flt	1722.6	1084.6	1568.1	1159.4
% departures	50	40	40	50

The statistical correlation coefficient between the latter two rows of numerical data in Table 4 is 0.21341 (weak positive).

(iv) At ATL, the average delay introduced by the algorithm appears somewhat to depend on the ratio of departures to arrivals within the sample. Specifically, for the computations with the runway separation enforced at full scale, 1.0, the relevant data from Table 3 are reproduced in Table 5.

Table 5: The data on average delay and percentage of departures at ATL with runway fully enforced.

	Nov. 20, 2015	**Nov. 27, 2015**	**Nov. 28, 2015**	**Nov. 29, 2015**
Avg. delay/flt	2843.0	963.4	721.4	1437.6
% departures	70	50	50	50

The statistical correlation coefficient between the latter two rows of numerical data in Table 5 is 0.94960. Although such a value of the correlation coefficient is generally considered strong, it is based in this case on limited data and cannot serve as convincing evidence of an interdependence.

The phenomenological difference between LAX and ATL outlined in statements (iii) and (iv) may be caused by the difference in route network topology, traffic patterns, and ATO practices between the two airports.

(v) At CLT, the average delay per flight introduced by the algorithm for runway separation scale 1.0 ranged from 142.6 to 221.1 seconds (approximately from 2.4 to 3.7 minutes). A delay on the order of minutes is not significant in the sense that it is at least one order of magnitude less than the duration of even a short fight. Consequently, the data indicate that the actual flights proceeded at separation standards close to those in Table 2.

A possible explanation for the phenomena for statements (i) and (ii) is that air travel subsides on the day of the holiday, as most passengers have already arrived at their holiday destination and are not yet departing. Evidentiary support for this explanation can be seen in Table 6. The Table shows the total operation counts at the airport, taken on the same day of the week in: the holiday week, the four weeks immediately preceding the holiday, and the week following the holiday. At each of the examined three airports (LAX, ATL, CLT), the operational count on the day of the holiday is substantially lower than those in the other weeks on the same day of the week.

Table 6: Comparison between air travel (by operation count) on a holiday and on non-holidays on the same day of the week. The holiday dates are marked with an *. Data source: FAA OPSNET.

LAX		ATL		CLT	
Date	**Total Operation Count**	**Date**	**Total Operation Count**	**Date**	**Total Operation Count**
2014-06-06	1,875	2013-10-31	2,400	2013-10-31	1,581
2014-06-13	1,916	2013-11-07	2,568	2013-11-07	1,636
2014-06-20	1,931	2013-11-14	2,597	2013-11-14	1,696
2014-06-27	1,916	2013-11-21	2,593	2013-11-21	1,657
*2014-07-04	1,572	*2013-11-28	1,638	*2013-11-28	847
2014-07-11	1,959	2013-12-05	2,461	2013-12-05	1,545

VI. Conclusions and Future Work

The algorithm presented in Section III is aimed at addressing aircraft separation for a collective of aircraft in flight within a given zone (comparable in size with the terminal airspace). A key assumption is that the flights have been sequenced and routed. Each flight is to commit to a speed profile provided by the flight's FMS. The output of the algorithm can be corrected for perturbations to the execution of the speed profile and to departure times using the methodology described in Appendix A. The main goal of the algorithm is to provide automated support for separation assurance that, according to the FAA requirements, must be maintained continuously at all times.

Numerical experiments, described in Section IV and summarized in Section V, suggest that the current implementation of the algorithm succeeds at keeping the aircraft separated according to the required standards. At the same time, the numerical evidence indicates that the algorithm generally introduces excess separation (resulting in flight delay). This delay can be reduced or removed by modeling more accurately the separation practices for separating arriving aircraft at the runway. The dependence of the amount of this excess delay on the ratio of departures to arrivals within a given operation cannot, in the authors' opinion, be clearly characterized from the above results and requires further research.

In the above algorithm, the sequence in which the flights enter the commitment zone was assumed given. If the sequence is not given and must be computed as part of the algorithm, then the problem (regarding the flights as the nodes, and the time separations $\triangle t$ as distances) becomes an Asymmetric Traveling Salesman Problem [21], further complicated by two circumstances: the distances may not conform to the triangle inequality, and the possibility of multiple flights lined up on the same route impose additional constraints, known in the literature as *precedence constraints* [12].

Among the possible directions of further research are: methods of addressing the sources of error described in Section IV.D, a refinement of the separation requirements to remove the excessive excessive constraints and obtain more accurate estimates of delay, and a number of computations in which the intended speed profiles are perturbed, leading to a need to run the algorithm again.

Consideration of how the algorithm, when refined for use in the field, might be implemented highlights two requirements in data communication. One is that the computer on which the algorithm is run must be able to receive sufficiently early the intent (computed by the FMS) of all the aircraft involved. The second requirement is that the times of entry into the commitment zone, when they have been computed, must be conveyed to the corresponding flights. Only one numerical value per flight need be broadcast.

VII. Acknowledgments

We thank the following colleagues: NASA - J. Jung, C. Gong, D. Isaacson, J. Robinson, M. Eshow, H. Tang; Intrinsyx - S. Ranjan, M. Lui; Science Applications International Corporation - W. Preston, J. Cisek; University Affiliated Research Center - S. Rangoon, L. Chen, G. Wu; State University at Stony Brook - J. Mitchell.

A. Sensitivity to perturbations of the speed profile and of the departure times

Suppose an aircraft is to fly along its route with arc length coordinate s. In general, the ground speed profile $v(s)$ to which that aircraft is committed in region C is not executable exactly, but will rather experience perturbations (e.g., caused by the wind). If $\epsilon(s)$ denotes the perturbation (e.g., caused by wind) to the aircraft's execution of the speed profile $v(s)$ at position s, then the kinematic equation describing the motion of the aircraft along its route is

$$\frac{ds}{dt} = v(s) + \epsilon(s).$$

The question central to this Appendix is as follows: if the aircraft starts in position $s^{(1)}$ at time $t^{(1)}$ and in the absence of perturbations ($\epsilon \equiv 0$) reaches position $s^{(2)}$ at time $t^{(2)}$, how will the perturbation $\epsilon(s)$ affect the time $t^{(2)}$ (changing it to a time $t^{(2),\epsilon}$) of reaching position $s^{(2)}$?

To answer this question, solve the latter differential equation for dt and integrate from $t^{(1)}$ to $t^{(2)}$ for the unperturbed case,

$$t^{(2)} - t^{(1)} = \int_{t^{(1)}}^{t^{(2)}} dt = \int_{s^{(1)}}^{s^{(2)}} \frac{ds}{v(s)},$$

and also for the perturbed case,

$$t^{(2),\epsilon} - t^{(1)} = \int_{t^{(1)}}^{t^{(2),\epsilon}} dt = \int_{s^{(1)}}^{s^{(2)}} \frac{ds}{v(s) + \epsilon(s)}. \tag{6}$$

The above question asks what the difference is between $t^{(2),\epsilon}$ and $t^{(2)}$. An exact expression for this difference will now be obtained in terms of the difference between the integrands on the right-hand sides of the latter two equations. Expand the latter integrand in powers of $\epsilon(x)$:

$$\frac{1}{v(s) + \epsilon(s)} = \frac{1}{v(s)} \left(\frac{1}{1 + \epsilon(s)/v(s)} \right) = \frac{1}{v(s)} \sum_{m=0}^{\infty} \left(-\frac{\epsilon(s)}{v(s)} \right)^m.$$

Consequently, the difference between the integrands $1/(v(s) + \epsilon(s))$ and $1/v(s)$ is

$$\frac{1}{v(s)} \sum_{m=1}^{\infty} \left(-\frac{\epsilon(s)}{v(s)} \right)^m = -\frac{\epsilon(s)}{v(s)^2} + \frac{\epsilon(s)^2}{v(s)^3} + \Big(\text{higher powers of } \epsilon(s)\Big), \tag{7}$$

and the change in $t^{(2)}$ that results from the perturbation is

$$t^{(2),\epsilon} - t^{(2)} = \int_{s^{(1)}}^{s^{(2)}} \left[-\frac{\epsilon(s)}{v(s)^2} + \frac{\epsilon(s)^2}{v(s)^3} + \Big(\text{higher powers of } \epsilon(s)\Big) \right] ds.$$

If the absolute perturbation $|\epsilon(s)|$ is at every s smaller than $|v(s)|$[b] (thus guaranteeing convergence of the power series), then the latter expression in square brackets can be bounded using the following facts from calculus:

- In the special case $\frac{\epsilon(s)}{v(s)} > 0$, the power series $\sum_{m=1}^{\infty} (-\epsilon(s)/v(s))^m$ in (7) is an alternating series. Therefore, the M-th partial sum

  $$\sum_{m=1}^{M} \left(-\frac{\epsilon(s)}{v(s)} \right)^m$$

  approximates the sum of the series with an error not exceeding $|\epsilon(s)/v(s)|^{M+1}$.

- In the general case, the approximation error for the M-th partial sum equals

  $$\begin{aligned} \textstyle\sum_{m=1}^{\infty} \left(-\frac{\epsilon(s)}{v(s)} \right)^m - \sum_{m=1}^{M} \left(-\frac{\epsilon(s)}{v(s)} \right)^m &= \textstyle\sum_{m=M+1}^{\infty} \left(-\frac{\epsilon(s)}{v(s)} \right)^m \\ &= \left(-\frac{\epsilon(s)}{v(s)} \right)^{M+1} \textstyle\sum_{n=0}^{\infty} \left(-\frac{\epsilon(s)}{v(s)} \right)^n \\ &= \left(-\frac{\epsilon(s)}{v(s)} \right)^{M+1} \frac{1}{1+(\epsilon(s)/v(s))}, \end{aligned}$$

  where the last equality follows from the formula for the sum of a convergent geometric series.

[b] The precise statement would be $|\epsilon(s)/v(s)| \leq$ (some constant independent of s) < 1 for all s.

The computed expression for the correction of $t^{(2)}$ for the perturbation $\epsilon(s)$ gives time buffers by which one may wish to "pad" the time separations $\triangle t$ in (2).

A way to correct also for perturbations to the departure times is to introduced an additive error term to the right-hand side of equation (6) in the Appendix:

$$t^{(2),\epsilon} - t^{(1)} = \int_{s^{(1)}}^{s^{(2)}} \frac{ds}{v(s) + \epsilon(s)} + \text{(error in the departure time for that flight)},$$

which gives the worst-case bound

$$\left| t^{(2),\epsilon} - t^{(1)} \right| \leq \left| \int_{s^{(1)}}^{s^{(2)}} \frac{ds}{v(s) + \epsilon(s)} \right| + \text{(upper bound on the error in the departure time for that flight)}.$$

References

[1] D. R. Isaacson, A. V. Sadovsky, and D. Davis. Scheduling for Precision Air Traffic Operations: Problem Definition and Review of Prior Research. *Journal of Aerospace Information Systems*, 11:234–257, 2014.

[2] Air Traffic Control Order JO 7110.65U. *U.S.A. Federal Aviation Administration*. U.S. Dept. of Transportation, Washington, D.C., 2012.

[3] D. R. Isaacson, J. E. Robinson III, H. Swenson, and D. Denery. A concept for robust, high density terminal air traffic operations. In *10th AIAA Aviation Technology, Integration, and Operations (ATIO) Conference, Fort Worth, TX*, 2010.

[4] A. V. Sadovsky, D. Davis, and D. R. Isaacson. Separation-compliant, optimal routing and control of scheduled arrivals in a terminal airspace. *Transportation Research Part C: Emerging Technologies*, 37(0):157 – 176, 2013. URL: http://www.sciencedirect.com/science/article/pii/S0968090X13002064, doi:http://dx.doi.org/10.1016/j.trc.2013.09.017.

[5] A. Rezaei, A.V. Sadovsky, J. Speyer, and D.R. Isaacson. Separation-compliant speed control in terminal airspace. In *AIAA-2013-4781, AIAA Guidance, Navigation, and Control (GNC) Conference, Boston, MA*, 2013.

[6] A. V. Sadovsky, D. Davis, and D. R. Isaacson. Efficient computation of separation-compliant speed advisories for air traffic arriving in terminal airspace. *Journal of Dynamic Systems, Measurement, and Control*, 136, 2014.

[7] D. R. Isaacson and A. V. Sadovsky. *Schedule Dissimilarity and Stability Metrics for Robust Precision Air Traffic Operations*. NASA-TM-2014-216618, 2014.

[8] A.V. Sadovsky and B.C. Fabien. Separation-compliant time advance in terminal area arrivals: Tradeoff between makespan and fuel burn. In *AIAA Guidance, Navigation, and Control (GNC) Conference, Boston, MA*, 2013.

[9] A.V. Sadovsky, H.N. Swenson, W.B. Haskell, and J. Rakas. Optimal time advance in terminal area arrivals: Throughput vs. fuel savings. In *30th Digital Avionics Systems Conference (DASC), Seattle, WA*, 2011.

[10] M. Xue and S. Zelinski. Optimal integration of departures and arrivals in terminal airspace. *Journal of Guidance, Control, and Dynamics*, 37:207–213, 2014.

[11] M. A. Konyak, D. Warburton, J. Lopez-Leones, and P. C. Parks. A Demonstration of an Aircraft Intent Interchange Specification for Facilitating Trajectory-Based Operations in the National Airspace System. In *AIAA Guidance, Navigation and Control Conference and Exhibit*, August 2008.

[12] N. Ascheuer, M. Jünger, and G. Reinelt. A Branch & Cut Algorithm for the Asymmetric Traveling Salesman Problem with Precedence Constraints. *Computational Optimization and Applications*, 17(1):61–84, 2000. doi:10.1023/A:1008779125567.

[13] B. G. Sokkappa. The Impact of Metering Methods on Airport Throughput. *Journal of Air Traffic Control*, 31:45–48, 1989.

[14] H. Erzberger. CTAS: Computer Intelligence for Air Traffic Control in the Terminal Area, 1992.

[15] W. Nedell, H. Erzberger, and F. Neuman. The traffic management advisor. 1990.

[16] A.M. Bayen and C.J. Tomlin. Real-time discrete control law synthesis for hybrid systems using milp: application to congested airspace. In *American Control Conference, 2003. Proceedings of the 2003*, volume 6, pages 4620–4626, June 2003. doi:10.1109/ACC.2003.1242452.

[17] W.P. Niedringhaus. Stream option manager (som): automated integration of aircraft separation, merging, stream management, and other air traffic control functions. *Systems, Man and Cybernetics, IEEE Transactions on*, 25(9):1269–1280, Sep 1995. doi:10.1109/21.400505.

[18] B. Kotnyek. An annotated overview of dynamic network flows. *CCSd/HAL: e-articles server (based on gBUS) [http://hal.ccsd.cnrs.fr/oai/oai.php] (France)*, 2003.

[19] C. D. Arendt. *Optimal control of fully routed air traffic in the presence of uncertainty and kinodynamic constraints*. PhD thesis, The Air Force Institute of Technology, 2014.

[20] H. Tang. Conflict Alerts for Aircraft on Visual Approaches. June 2015.

[21] C. H. Papadimitriou and K. Steiglitz. *Combinatorial Optimization; Algorithms and Complexity*. Dover Publications, 1998.